Journal of Nepal Geological Society, 2001, Vol. 25 (Sp. Issue), pp. 135–155

Geology, geochemistry, and radiochronology of the Kathmandu and Gosainkund Crystalline nappes, central Nepal Himalaya

Santa Man Rai

Department of Geology, Tribhuvan University, Tri-Chandra Campus, Kathmandu, Nepal
(Corresponding author, e-mail: geologytc@wlink.com.np)

ABSTRACT

A multidisciplinary study was carried out in the Lesser Himalaya (LH), the Kathmandu Crystalline Nappe (KCN) and the Gosainkund Crystalline Nappe (GCN) in central Nepal Himalaya. Two principal deformations are recorded in both the crystalline nappes and the Lesser Himalaya: ductile, syn-MCT/or syn-MT metamorphic deformation marked by microstructures (stretching lineation, S-C structures, and isoclinal folding) and post-MCT/or post-MT metamorphic deformation recorded by a major EW-directed Likhu Khola anticline and by NNE-SSW-directed folds. The Upper Lesser Himalayan rocks close to the Main Central Thrust (MCT) record syn-MCT metamorphic conditions at 750 MPa and 566 °C. The rocks of the KCN record P-T condition from 900 to 720 MPa and 700 to 484 °C, while the GCN rocks were equilibrated at upper amphibolite- to granulite-facies conditions from 890 to 583 MPa and 754 to 588 °C. The P-T conditions and field observations exhibit well-preserved inverted metamorphism between the Upper Lesser Himalaya and the Gosainkund Crystalline Nappe.

The augen gneisses from the GCN yielding 486±9 Ma U-Pb zircon age and the granites of similar age in the KCN bear similar petrographic and geochemical characteristics and suggest a similar magmatic origin although they belong to different tectonic units. The chemical analyses of the Proterozoic Ulleri augen gneiss of the LH and the granites of the KCN fall within the same compositional field, indicating a magmatic origin of these augen gneisses.

$^{40}Ar/^{39}Ar$ datings on muscovite indicate cooling ages younging systematically from south to north: 22 to 14 Ma in the KCN, 16 to 5 Ma in the GCN, and 12 to 6 Ma in the LH. This systematic younging of muscovite ages does not have any correlation with the present elevation, lithology and tectonic unit and is interpreted as a result of the exhumation of the rock units on the Main Himalayan Thrust (MHT) ramp situated to the north of Kathmandu Valley. Both the KCN and the GCN record a late emplacement history, but the KCN was exhumed earlier than the GCN. The two crystalline nappes presently form a single tectonic block, and the combined uplift of the two nappes occurs on a ramp of a major décollement developed in the upper part of the Indian crust.

INTRODUCTION

The Indian and the Eurasian continents collided in the Eocene time, which resulted in the development of the Himalayan mountain range. Due to the continued movement, the northern edge of the Indian crust was sheared and thrust to the south along a series of north-dipping thrust faults that divide the Himalayan orogen into three major intra-continental thrust packages (Gansser 1964; Schelling and Arita 1991). The Higher Himalayan Crystallines (HHC), also known as the Tibetan Slab, consist of amphibolite- to granulite-facies rocks, and are separated from the overlying Cambro-Ordovician to Eocene Tethyan Sedimentary Series (TSS) by a normal fault generally known as the South Tibetan Detachment System (STDS) (Burg et al. 1984; Burchfiel and Royden 1985; Pêcher 1991). Further south, the Main Central Thrust (MCT) carries the HHC over the low-grade (greenschist to lower amphibolite facies) metasedimentary rocks of the Lesser Himalaya. The Lesser Himalaya (LH) is thrust over the Mio-Pleistocene Siwalik rocks of a foreland basin along the Main Boundary Thrust (MBT). The Himalayan Frontal Thrust (HFT) is the youngest and the southernmost thrust system of the Himalaya, and forms a boundary between the Quaternary sediments of the Indo-Gangetic plain and the Siwalik rocks.

Many geoscientists have worked in the Kathmandu and Gosainkund Region since long time (Bordet et al. 1959; Gansser 1964; Hagen 1969; Arita et al. 1973, 1997; Stöcklin and Bhattarai 1977; Stöcklin 1980; Le Fort et al. 1983; Le Fort and Rai 1999; Inger 1991; Macfarlane et al. 1992; Macfarlane 1993, 1995; Morrison and Olivier 1992; Reddy et al. 1993; Pandey et al. 1995; Rai et al. 1997a, b; Rai 1998; Rai et al. 1998a,b, c; Upreti and Le Fort 1999; Johnson and Rogers 1997; Johnson et al. 2001). The HHC and the rocks of the Kathmandu Complex (Stöcklin and Bhattarai 1977; Stöcklin 1980; Arita et al. 1997; Johnson et al. 2001) are generally interpreted to be a single tectonic unit which is thrust over the LH along the Mahabharat Thrust (MT). The MT is considered as a southward prolongation of the MCT (Stöcklin 1980; Pandey et al. 1995; Johnson et al. 2001). However, the recent works by Rai et al. (1998c), Upreti and Le Fort (1999), and Upreti (1999) point to the existence of two different nappes, which are distinguished by their lithostratigraphy and metamorphism along a Kathmandu-Gosainkund transect. They recognise the KCN in the south and the GCN in the north which are separated by the MCT lying on the north side of the Kathmandu Valley. The GCN is a southward extension of the Higher Himalayan Crystallines in the Langtang Region. The GCN consists of amphibolite-to granulite-facies metamorphic rocks while the KCN constitutes the greenschist to amphibolite-facies rocks.

The aim of this paper is to present the geology, geochemistry, geochronology and metamorphism of the rocks in the study area and discuss the tectonic history of the Kathmandu and Gosainkund Crystalline nappes.

GEOLOGICAL SETTING

The area (longitude 84°30' and 85°45'; latitude 27°30' and 28°15') under study extends for about 80 km from south to north (from the East Rapti River to the Gosainkund Range) and 70 km from east to west (from the Indrawati to the Trisuli rivers) (Fig. 1). Three tectonic units are exposed in the area. From south to north, they are the Lesser Himalaya (LH), the Kathmandu Crystalline Nappe (KCN) and the Gosainkund Crystalline Nappe (GCN) (Fig. 2). The Miocene Nardanda pegmatite exposed in the northern margin of the Kathmandu Valley separates the GCN from the KCN. The KCN and the LH form the large ESE-WNW trending Mahabharat Synclinorium (Stöcklin and Bhattarai 1977; Stöcklin 1980). The lithostratigraphy of the LH, KCN and GCN were compared by Upreti and Le Fort (1999).

Lesser Himalaya (LH)

In central Nepal, the LH is divided into two groups: the Lower Lesser Himalaya and the Upper Lesser Himalaya (Le Fort 1975; Pêcher 1978; Colchen et al. 1980, 1986) or the Lower Nawakot Group and Upper Nawakot Group (Stöcklin and Bhattarai 1977; Stöcklin 1980). This unit is composed of late Precambrian to Paleozoic? sedimentary and metasedimentary rocks such as limestone, dolomite, gritstone, conglomerate, slate, phyllite, schist, metasandstone, quartzite, augen gneiss (Ulleri augen gneiss) and amphibolite. These rocks are exposed around the Kathmandu Valley (Fig. 3). The upper section of the Upper Lesser Himalaya along the Mailung Khola in the vicinity of the MCT has undergone strong deformation, and metamorphosed to amphibolite-facies producing garnet and/or kyanite related to the movement along the MCT (Le Fort 1975, Pêcher 1978, 1989), while only greenschist-facies rocks can be observed at the proximity of the MT (Fig. 3).

Kathmandu Crystalline Nappe (KCN)

This nappe is composed of the rocks of the Kathmandu Complex, which is divided into the Bhimphedi and Phulchauki groups (Stöcklin and Bhattarai 1977; Stöcklin 1980). The

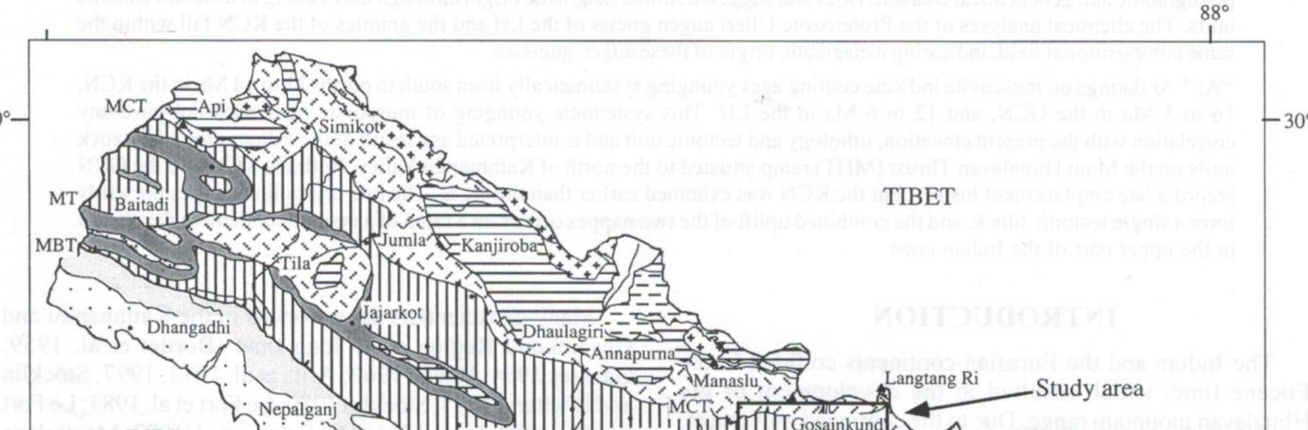

Fig. 1: Geological map of Nepal (after Upreti and Le Fort 1999). HH leucogranite: Higher Himalayan leucogranite, HHSS Mesozoic: Tethyan Sedimentary Series (Mesozoic) of the Higher Himalaya, HHSS Paleozoic: Tethyan Sedimentary Series (Paleozoic) of the Higher Himalaya, LH crystalline nappe: Lesser Himalayan crystalline nappe, LH granite: "Lesser Himalayan" granite, LH Paleozoic: Sedimentary Series (Paleozoic) of the Lesser Himalayan nappes (Phulchauki Group), MBT: Main Boundary Thrust, MCT: Main Central Thrust, MT: Mahabharat Thrust, STDS: South Tibetan Detachment System.

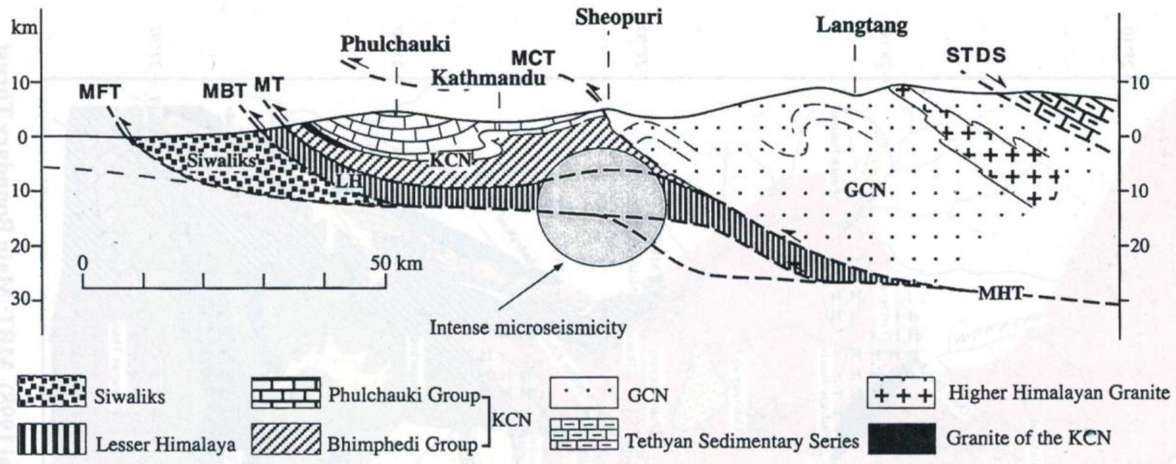

Fig. 2: Section across the central Nepal nappes (after Upreti and Le Fort 1999) with the localisation of the present intense microseismicity (after Pandey et al. 1995). GCN: Gosainkund Crystalline Nappe, KCN: Kathmandu Crystalline Nappe, LH: Lesser Himalaya, MBT: Main Boundary Thrust, MCT: Main Central Thrust, MFT: Main Frontal Thrust, MHT: Main Himalayan Thrust, MT: Mahabharat Thrust, STDS: South Tibetan Detachment System.

Bhimphedi Group is the lower unit and is composed of amphibolite-facies rocks (phyllite, schist, metasandstone, quartzite, and marble of Precambrian age). The metamorphic rocks of the Bhimphedi Group gradually pass upward to a low-grade to non-metamorphosed fossiliferous Lower Paleozoic sequence of Tethyan affinity belonging to the Phulchauki Group which is composed of limestone, slate, metasandstone, phyllite, calc-phyllite and marble. The rocks of the Kathmandu Complex are also intruded by several Cambro-Ordovician peraluminous granitic plutons (Le Fort et al. 1981, 1983; Schärer and Allègre 1983) in the south, east and west of the Kathmandu Valley. Small augen gneiss bodies of granitic origin are found in the Bhimphedi Group exposed along the Mahesh Khola, Malekhu Khola, Belkhu Khola and the Bagmati River. Along Malekhu Khola, incipient development of kyanite in this gneiss is also observed.

A 15 km long E-W running narrow pegmatite body named the Nardanda Pegmatite is exposed at the northern edge of the Kathmandu Valley. It has a maximum exposed thickness of 300 m at the middle part (Fig. 3).

Gosainkund Crystalline Nappe (GCN)

The Gosainkund Crystalline Nappe (GCN) lies to the north of the Kathmandu Valley and consists of the amphibolite-to granulite-facies rocks. The nappe reaches to the northern edge of the Kathmandu Valley, and extends up to Nagarkot in the east and to Galchi in the west (Fig. 3).

The high-grade metamorphic rocks of the GCN include varieties of paragneiss and orthogneiss (augen gneiss, granitic gneiss), micaschist, migmatite, calc-silicate gneiss, marble and quartzite (Fig. 3). The gneisses exposed along the higher part of the Sheopuri Range such as at Thakle, SW of Melamchi Bazaar and in the Gosainkund Range (Fig. 3), contain abundant sillimanite (Rai 1998). The lower sections of the GCN exposed along the Likhu and Tadi Kholas lying to the north of the Sheopuri Range contain kyanite-garnet bearing rocks, whereas sillimanite occurs at a higher section on both sides of these rivers.

STRUCTURE AND DEFORMATION

Major Thrusts

Main Central Thrust (MCT)

The MCT is a major post-collisional thrust fault traceable throughout most of the Himalayan range (Gansser 1964; Le Fort 1975; Pêcher 1989). Along the northern margin of the Kathmandu Valley, this thrust brings the rocks of the GCN over that of the KCN (Fig. 3). Along the Tadi Khola and Likhu Khola sections, the paragneiss at the base of the GCN is highly sheared, with the presence of quartz boudins and highly stretched garnets along the foliation plane. In the north of the Kathmandu Valley along the southern margin of the GCN, the MCT lies at the top of the Nardanda pegmatite.

In the Gosainkund-Kathmandu region, the MCT swings round from its general E-W trend and becomes N-S trend along the eastern and western areas. Between the Sheopuri Range and Gosainkund Range the thrust makes a bowl-shaped structure due to its dip due east, west and north (Fig. 4).

Mahabharat Thrust (MT)

The KCN is thrust over the LH along the MT (Stöcklin and Bhattarai 1977; Stöcklin 1980; Pandey et al. 1995; Arita et al. 1997; Johnson et al. 2001). These authors insist that the MT is a southward continuation of the MCT. However, some authors interpret the MT as a separate thrust fault (Rai 1998; Rai et al. 1998c; Upreti and Le Fort 1999; Upreti 1999). At the proximity of the MT, highly sheared ductile fabrics are visible at the base of the Raduwa Formation of the

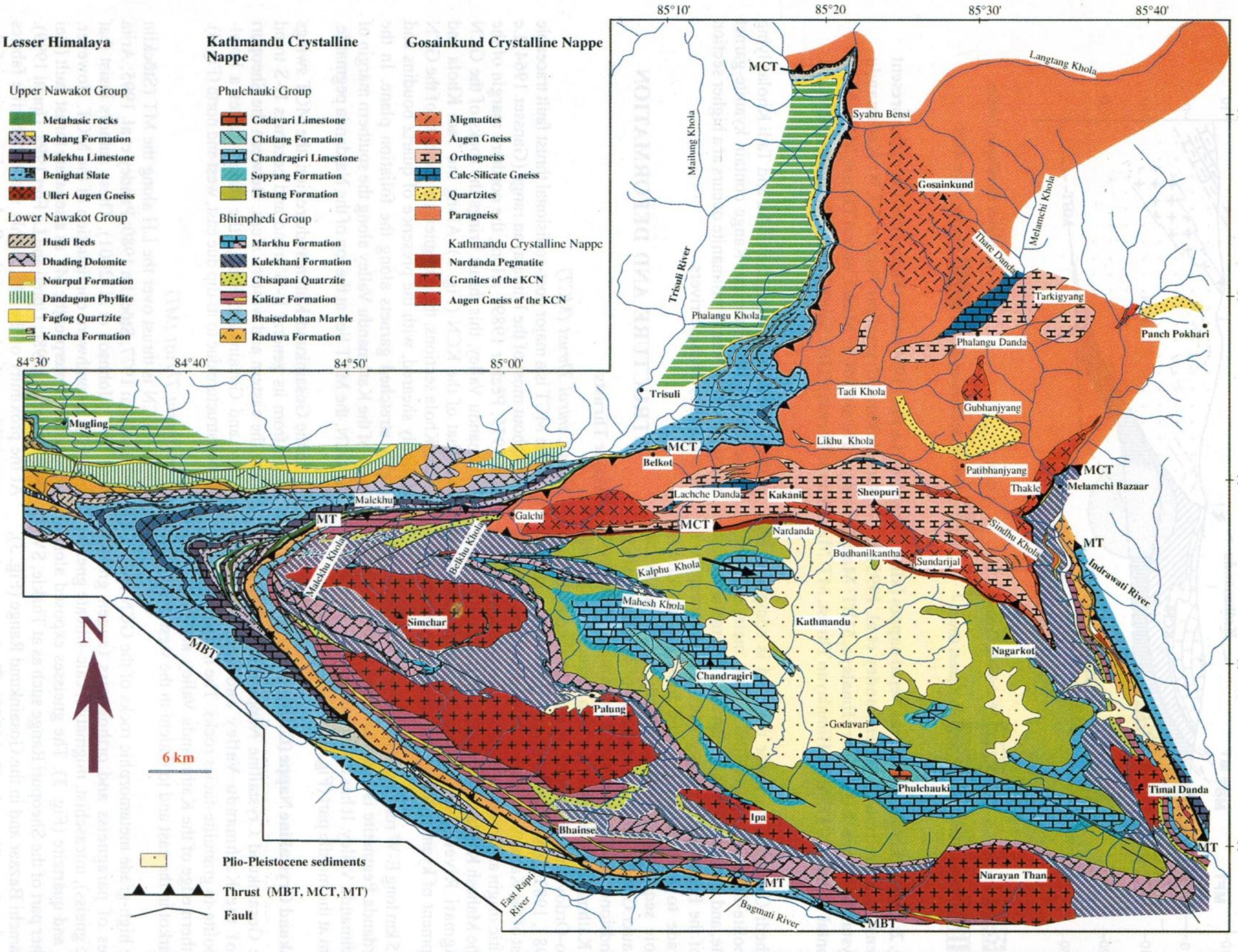

Fig. 3: Geological map of the study area in the central Nepal (after Stöcklin and Bhattarai 1977; Stöcklin 1980; Rai 1998). MBT: Main Boundary Thrust, MCT: Main Central Thrust, MT: Mahabharat Thrust.

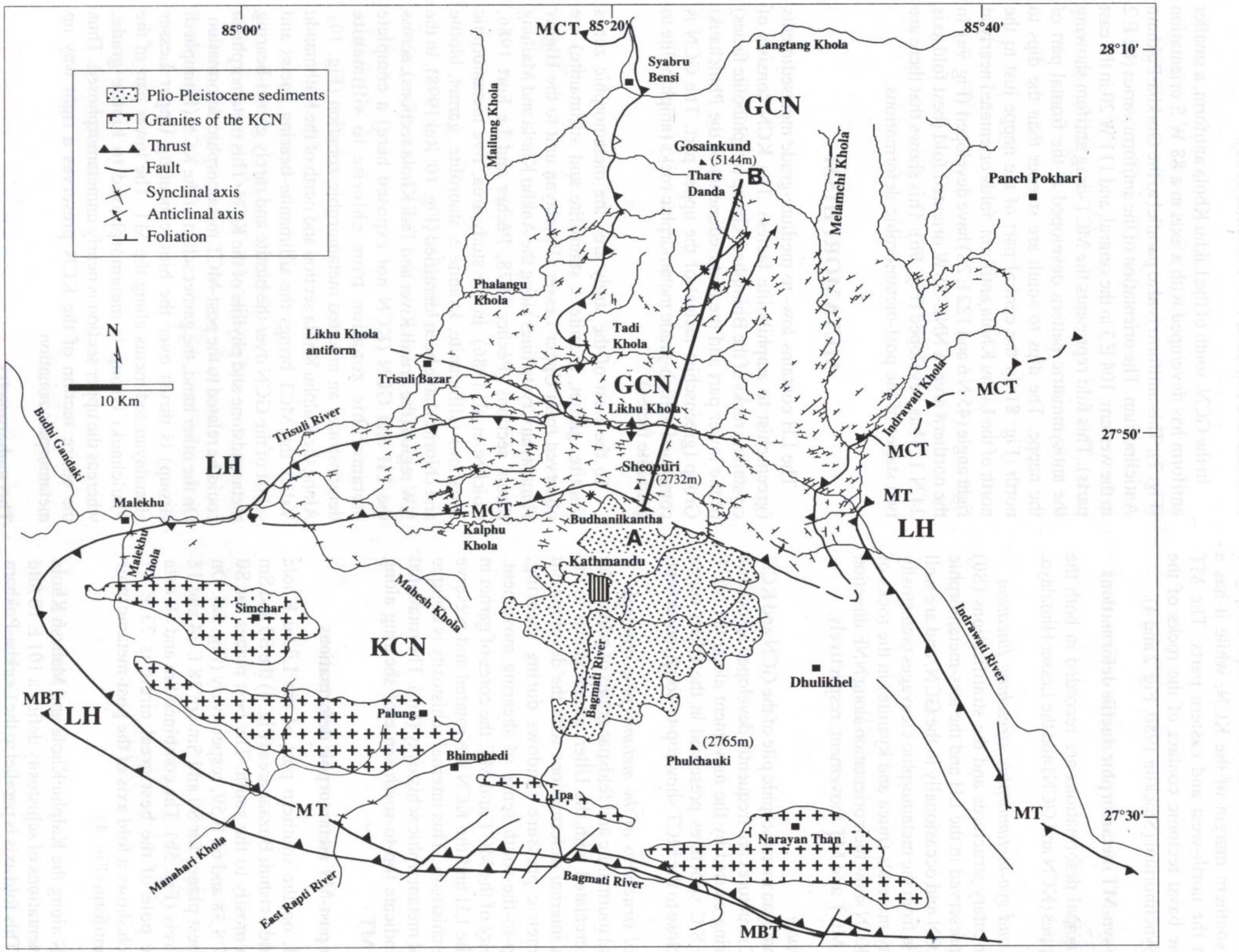

Fig. 4: Metamorphic foliation trajectory map of the study area, principally in the Gosainkund Crystalline Nappe. A-B represents the cross-section shown in Fig. 8. GCN: Gosinkund Crystalline Nappe, KCN: Kathmandu Crystalline Nappe, LH: Lesser Himalaya, MBT: Main Boundary Thrust, MCT: Main Central Thrust, MT: Mahabharat Thrust.

Bhimphedi Group. Highly stretched quartz segregations are parallel to the schistose foliation. The MT dips steeply to north at the southern margin of the KCN, while it has a gentle dip in the north-west and eastern parts. The MT constitutes the basal tectonic contact of the rocks of the Mahabharat Synclinorium (Stocklin 1980, Fig. 2 and 4).

Syn-MCT/or syn-MT metamorphic ductile deformations

Three principal deformations are recorded in both the crystalline nappes (KCN and GCN) and the Lesser Himalaya.

(i) Cleavage and syn-metamorphic stretching lineation
The sedimentary structures and the stratifications (S0) are still well preserved in the LH and the less-metamorphic parts of the KCN and occasionally in the GCN, and are well distinguishable from the metamorphic cleavages (schistosity Sm). The platy minerals (mica and kyanite) in the rocks of the GCN and KCN show their orientation along NNE direction related to the MCT and MT movement, respectively.

(ii) S-C structure
In the Himalayan metamorphic pile of the GCN and KCN rocks, the S-C structures are frequently developed associated with the shearing caused by the movement along the MCT and MT. The S-C structures preserved in the Ulleri augen gneiss found close to the MCT show top-to-south movement.

(iii) Rotational structures of the metamorphic minerals
The detrital tourmaline and feldspar grains of graywacke and schist intercalated with the Ulleri augen gneiss in the LH show less internal deformations with the development of the asymmetric pressure shadows during shearing, indicating top-to-the-south sense of shearing movement. At the proximity of the MCT and MT, the cores of garnet in the rocks of the LH and the KCN are rotated and preserve their internal schistosity. This internal schistosity is oblique to the principal metamorphic schistosity (Sm). The rotational garnets also indicate top-to-south sense of shearing along the MCT and MT.

Post-MCT/ or post-MT metamorphic deformations

In the LH, on the southern part of the Likhu Khola antiform around Trishuli Bazaar area (Fig. 4) the S0 and Sm of the LH dip mostly to the south. The best planes for S0 and Sm are 67 S 38 and 68 S 59, respectively (Fig. 5a). On the north the best planes for S0 and Sm are 38 E 34 and 18 E 23, respectively (Fig. 5b). The combined Sm and S0 data show that the pole of the best great circle is 73 E 17 (Fig. 5c), which shows a fold axis of the post-metamorphic Likhu Khola antiform (Fig. 4).

In the KCN along the Kalphu Khola and Mahesh Khola (Fig. 4), the orientations of schistosity define a 101 E 10 fold axis (Fig. 6a). This fold axis is parallel to the Gorkha-Pokhara Anticlinorium. A refolded structure, oriented along the NNE-SSW direction (24 N 5) is also observed (Fig. 6a). In the eastern part of the KCN (north of Dhulikhel), the schistosity pole defines a great circle oriented along 133 W 23 (Fig. 6b) which shows parallelism with the Mahabharat Synclinorium (Stöcklin and Bhattarai 1977; Stöcklin 1980).

In the GCN, south of the Likhu Khola antiform, a smaller antiform has developed with a axis in a 88 W 5 orientation (Fig. 7). This antiform is also parallel to the Gorkha-Pokhara Anticlinorium. The orientation of the antiform varies (82 E 2 in the western, 104 E 3 in the central, and 111 W 20 in the east parts). This fold represents the MCT-drag antifom showing the antisymmetric pattern developed at the frontal part of the nappe. The dips to south are steeper than the dips to north (Fig. 8). In the central part of the nappe just to the north of the Likhu Khola antiform, folds orientated nearly at right angle (45 N 6 and 122 E 28) have developed (Fig. 9a). In the northern area, a NNE-SSW oriented fold (best fold axis 24 N 12) has developed (Fig. 9b). This shows that there are two stages of the post-metamorphic deformations.

METAMORPHISM

The LH contains low- to medium-grade metasediments (greenschist to amphibolite facies). The KCN consists of crystalline rocks of the Bhimphedi Group (amphibolite facies) of the lower part and the metasediments of the Phulchauki Group (greenschist facies) of the upper part. The GCN is composed of high-grade metamorphic rocks (amphibolite to granulite facies).

To the west of the study area the metamorphic zones (biotite, garnet, kyanite ± staurolite and sillimanite) are observed from Upper Lesser Himalayan unit to the Higher Himalayan Crystallines along the Ankhu Khola and Mailung Khola sections (Pêcher 1978; Pêcher and Le Fort 1986; Colchen et al. 1986). In the study area, five metamorphic zonations (sillimanite, kyanite ± staurolite, garnet, biotite and chlorite) have been identified (Fig. 10; Rai 1998). In the NW region (the Trisuli River and Tadi Khola sections), across the LH and GCN (KCN not exposed here) a complete metamorphic zonation from chlorite to sillimanite demonstrates an inverted metamorphic zonation (Fig. 10). Along the Kalphu Khola section and north of the Kathmandu Valley the MCT brings the sillimanite-bearing gneiss and schist of the GCN over the biotite and rarely garnet-bearing metasandstone and phyllite of the KCN. This metamorphism could be related to the post-MCT metamorphic deformation. On the other hand, the garnet schist of the KCN (Bhimphedi Group) is thrust over the biotite bearing Upper Lesser Himalayan sediments along the MT. The lower part of the Phulchauki Group is metamorphosed to biotite grade, whereas the upper section is nearly unmetamorphosed. Thus the entire section of the KCN preserves a right way up metamorphic zonation.

Thermobarometry

Metamorphic pressure and temperature from schist and gneiss from all the three tectonic units were calculated using Thermocalc thermobarometric calibrations (Holland and

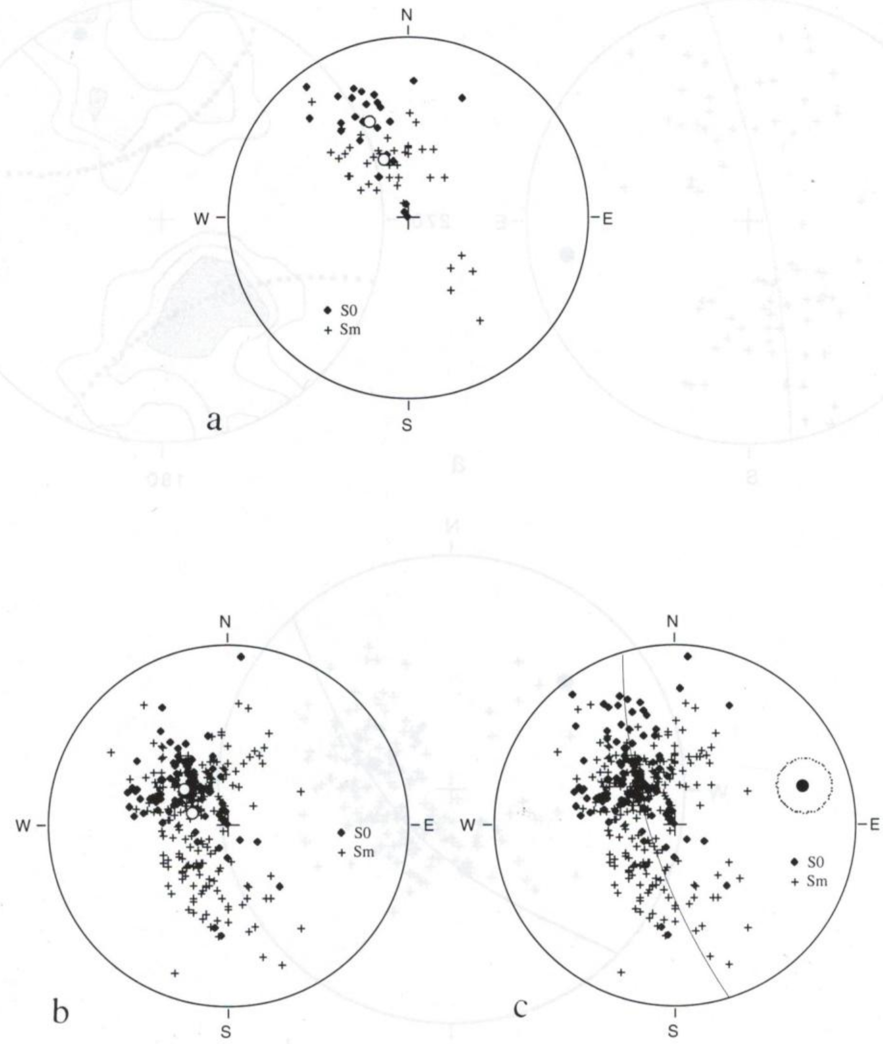

Fig. 5: a: Fabric diagram showing the poles of the S0 (stratification) and Sm (schistosity) in the southern flank of Likhu Khola antiform in the Lesser Himalaya (Fig. 4). Equilateral projection in the lower hemisphere of Wulff net (SchmidtMac programme, Pêcher, 1989a). Symbol: Solid circle = S0, cross = Sm. Best plane S0: 67 S 38, and best plane Sm: 68 S 59 (66 measures).

b: Fabric diagram showing the position of the S0 and Sm in the northern flank of the Likhu Khola antiform in the Lesser Himalaya. Solid circle = S0, cross = Sm. Best plane S0 : 38 E 34, Best plane Sm : 18 E 23.

c: Fabric diagram showing the whole measures of S0 and Sm in the Lesser Himalaya. Solid circle = S0, cross = Sm. Axis of the best great circle = 73 E 17.

Powel 1990). The P-T conditions of the upper LH, KCN and GCN samples are discussed in Rai et al. (1998c). The Upper Lesser Himalayan rocks close to the MCT record the syn-MCT metamorphic conditions at 750 ± 150 MPa and 566 ± 136 °C. The P-T values obtained from the rocks of the KCN widely vary. The rocks from the Bhimphedi Group at the proximity of the MT along the East Rapti River record a P-T conditions of 720 ± 420 MPa and 484 ± 194 °C. The rocks of the KCN exposed near the MCT that were collected at Melamchi Bazaar and near the Sindhu Khola show the P-T conditions 900 ± 140 MPa and 700 ± 60 °C.

The P-T conditions recorded from the GCN rocks are 890 ± 260 MPa to 583 ±198 MPa and 754 ± 40 °C to 588 ± 100 °C. The final equilibration of the upper section of the GCN occurred with a pressure and temperature drop of 170 MPa ± 100 MPa and 60 °C ± 20 °C respectively (using the core to rim differences).

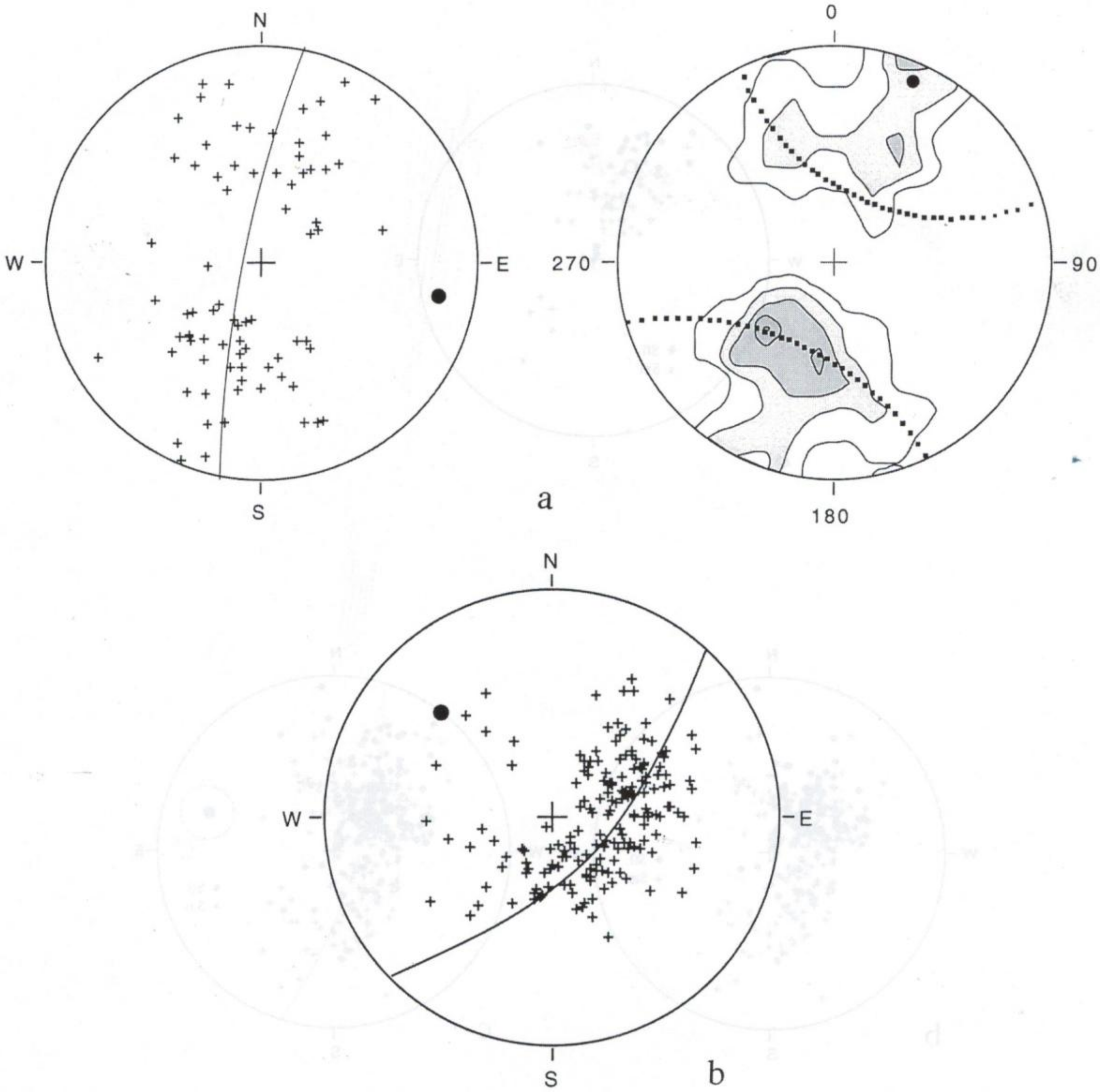

Fig. 6: a: Fabric diagram showing the position of the Sm in the central and western part of the Kathmandu Crystalline Nappe (west and north from Kathmandu City). Poles of the best great circle: 101 E 10 (left) and 24 N 5 (right) respectively (77 measures).
b: Poles of the Sm in the eastern part of the Kathmandu Crystalline Nappe (east from Kathmandu City). The pole of the best great circle: 133 W 23 (185 measures).

The estimated temperature in the KCN is lower by about 100 °C than that of the GCN, whereas the pressure remains at about 800 MPa in both the nappes.

GEOCHEMISTRY OF AUGEN GNEISSES AND GRANITE

Ulleri augen gneiss of the Lesser Himalaya

The Precambrian Ulleri augen gneiss has been reported along the Mailung Khola section (northwest of the Kathmandu Valley) lying at the top of the Kuncha Formation (Lower Nawakot Group) of the LH (Pêcher 1978). However, in the north of the Kathmandu Valley along the Phalangu Khola, Betrawati Khola, and near to the confluence of the Tadi Khola and the Likhu Khola, the Ulleri augen gneiss are exposed at the top of Benighat Slate (Upper Nawakot Group) of the LH (Fig. 3). They occur in the form of lenses and are highly deformed at the proximity of the MCT (Rai 1998; Le Fort and Rai 1999). It seems that there are two different units of the Ulleri augen gneisses in the LH occupying different stratigraphic levels. The gneiss is composed of medium-to coarse-grained of quartz, potash feldspar, plagioclase, biotite, muscovite and tourmaline. Biotite and muscovite defining the foliation planes are generally fine- grained and streaky

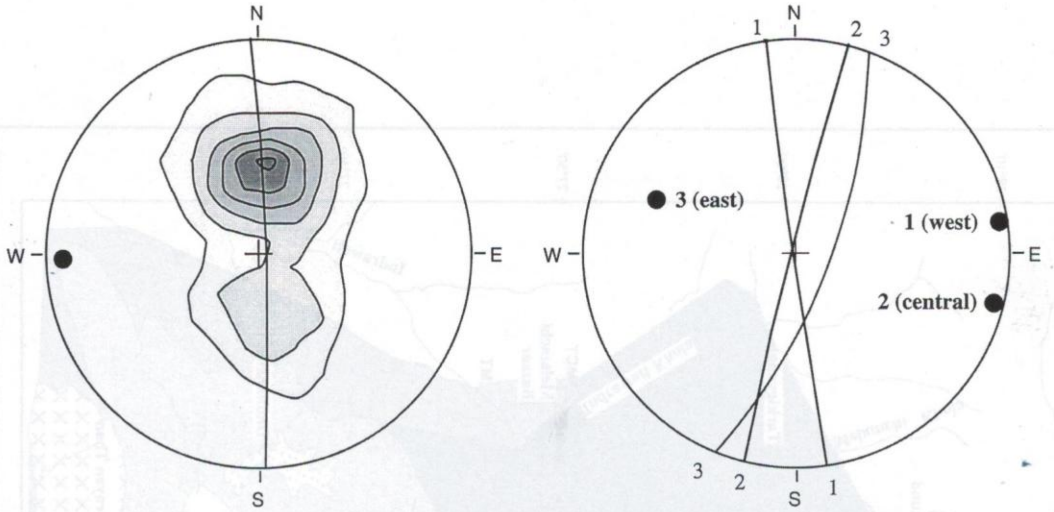

Fig. 7: Fabric diagram showing the position of Sm in the southern part of the Likhu Khola antiform in the Gosainkund Crystlline Nappe. Projection in the lower hemisphere of Wulff net (689 measures). At left, pole of best great circle: 88 W 5. At right, poles of the best great circles are in western part: 82 E 2 (1), central part: 104 E 3 (2) and eastern part: 111 W 20 (3), respectively.

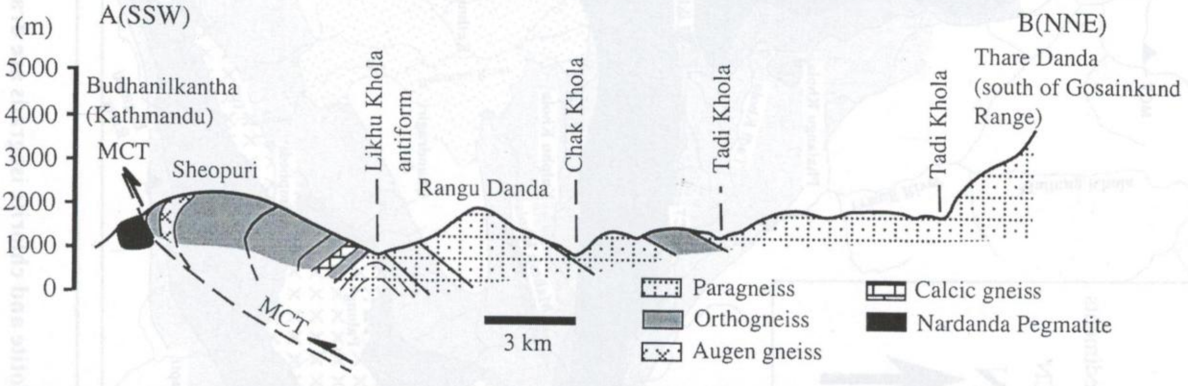

Fig. 8: Cross-section of the Gosainkund Crystalline Nappe between the northern edge of the Kathmandy Valley and Thare Danda (south of Gosainkund Range) (Fig. 4). MCT : Main Central Thrust.

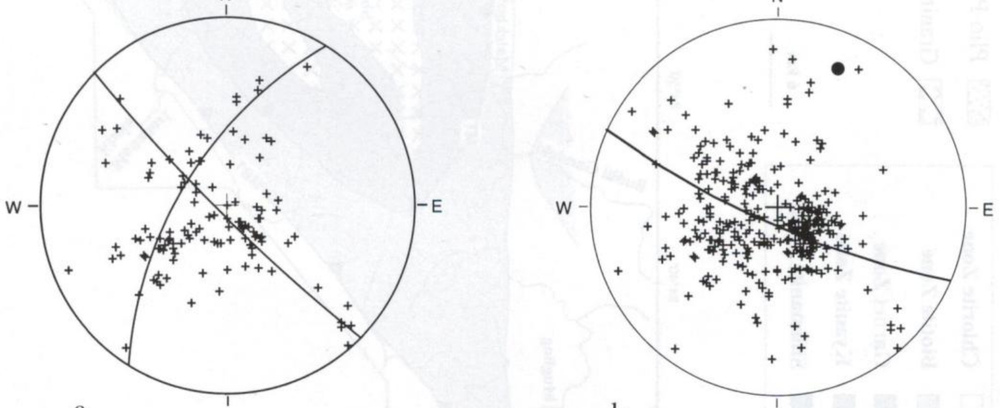

Fig. 9: a: Fabric diagram showing the position of the Sm in the central part of the Gosainkund Crystalline Nappe. Poles of the two large best circles are 45 N 6 and 122 E 28, respectively. Projection in the lower hemisphere of Wulff net (120 measures).

b: Fabric diagram showing the position of the Sm in the northern part of the Gosainkund Crystalline Nappe. Pole of the axis is 24 N 12. Projection in the lower hemisphere of Wulff net (348 measures).

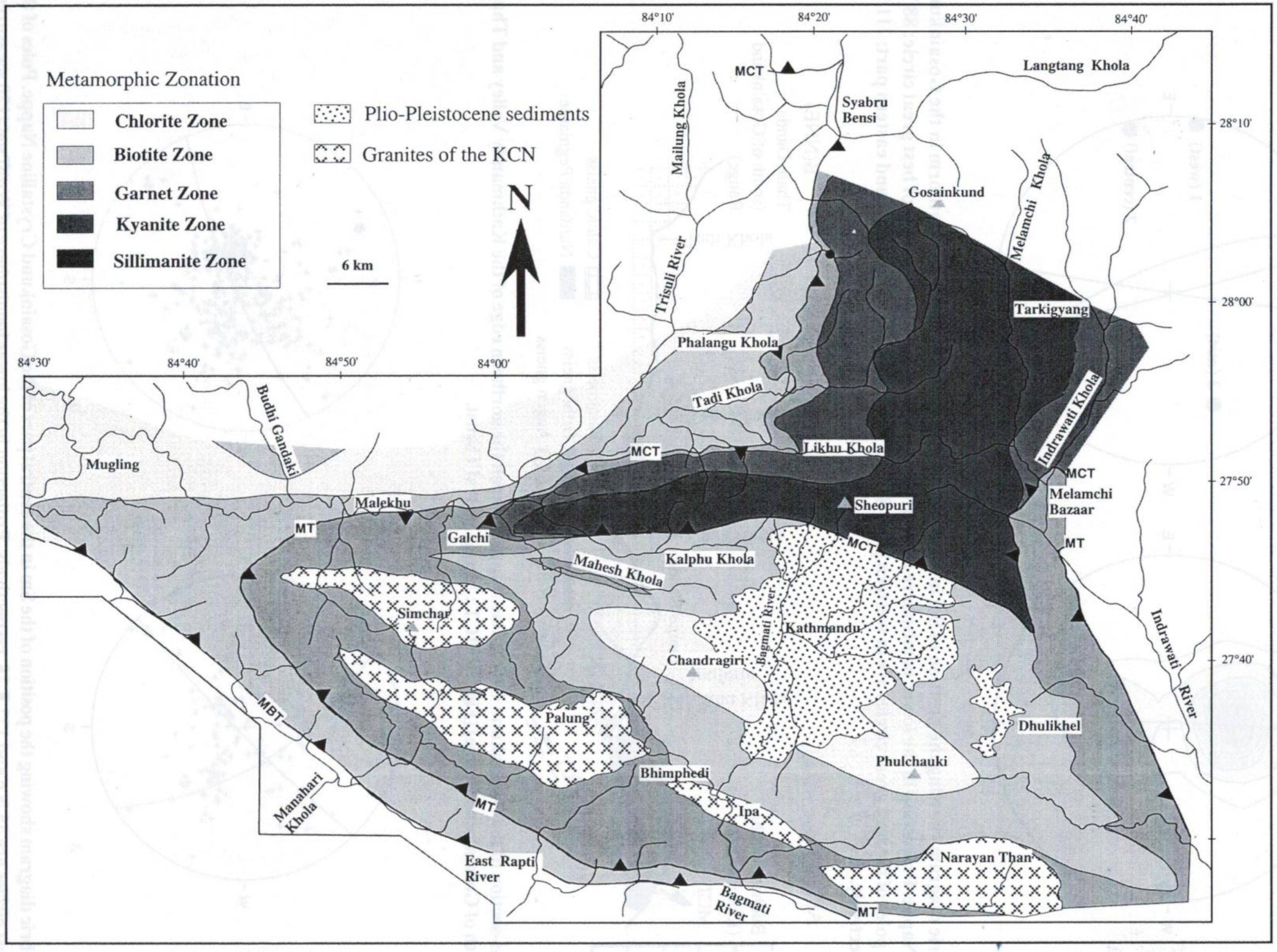

Fig. 10: Metamorphic zonation map of the study area. Biotite and chlorite isograds are drawn after Colchen et al. (1980) and Stöcklin (1980). MBT: Main Boundary Thrust, MCT: Main Central Thrust, MT: Mahabharat Thrust.

in nature imparting a very characteristic feature to the gneisses. These minerals constitute the regional metamorphic imprint on the gneiss, sometimes also marked by the recrystallization of garnets.

Geochemistry

The chemical composition of the gneiss is plotted in the diagram of the chemical-mineralogical classification of the common plutonic rocks and its magmatic associations prepared by Debon and Le Fort (1983, 1988). In this classification the nomenclature of the rocks with particular mineral, chemistry and magmatic association type can be determined. The geochemical characteristics of the Ulleri augen gneiss is compared with the granite of the KCN to determine its origin, though they belong to different tectonic units.

The chemical composition of three samples of the Ulleri augen gneiss is shown in Table 1. In the Q-P nomenclature diagram of Debon and Le Fort (1983, 1988) the composition of augen gneisses falls in the field of true granite, adamellite and granodiorite (Fig. 11). The rocks are peraluminous and correspond to two micas sectors of the A-B diagram (Fig. 12). In the Q-B-F diagram they show large variation in quartz (Q% - 35 to 48), dark minerals (B% - 5 to 13) and feldspars + muscovite (F% - 46 to 52) contents (Fig. 13). They are mainly leucocratic to subleucocratic with large variation in the K/(Na+K) ratio (Fig. 14). The chemical composition and petrographic characteristics of the Ulleri augen gneiss indicate a magmatic origin.

Augen gneiss of the Kathmandu Crystalline Nappe

Lenticular bodies of augen gneiss up to 50 m in thickness are exposed in different formations of the KCN along the Mahesh Khola, Belkhu Khola, Malekhu Khola and Bagmati River (Fig. 3). These are mainly exposed in the Bhimphedi Group. The augen gneiss is regarded as the metamorphosed small lenticular granite bodies. The recent U-Pb age determinations of zircons from these augen gneisses (Mahesh Khola) gave 471+12/-10 to 423±41 Ma (Johnson et al. 2001) which is very close to the ages of the granites from the KCN (discussed below).

Table 1: Chemical and mineralogical compositions of the Ulleri augen gneiss (Lesser Himalaya) and augen gneiss of the Kathmandu Crystalline Nappe. Analyses by emission spectrometry (K. Govindaraju, CRPG-CNRS, Nancy, except samples KN217, KN237 and LO202 by XRF at Geoscience Laboratory, GSP, Islamabad, Pakistan (where totals are rounded up to 100%) (Le Fort and Rai 1999). The parameters and topology are based on Debon and Le Fort (1983, 1988).

Ulleri augen gneiss					Kathmandu Crystalline Nappe					
Sample number	KN217	KN237	LO202	average	KN280	KN 288	KN295	KN301	KN481	average
SiO_2	71.70	78.22	72.21	74.04	74.86	74.12	73.20	72.84	75.02	74.01
Al_2O_3	13.92	12.23	14.49	13.55	12.87	13.49	13.07	13.29	13.28	13.20
$Fe_2O_3{}^t$	3.38	1.37	2.18	2.31	2.40	1.86	3.30	3.09	2.11	2.55
MnO	0.02	0.01	0.00	0.01	0.02	0.03	0.05	0.05	0.04	0.04
MgO	0.96	0.35	1.36	0.89	0.41	0.55	1.18	1.03	0.57	0.75
CaO	0.47	0.19	1.15	0.61	0.51	0.83	1.30	1.07	0.76	0.89
Na_2O	2.72	2.00	3.06	2.59	2.30	2.24	2.05	2.70	1.79	2.22
K_2O	5.23	4.77	2.90	4.31	5.57	5.74	4.56	4.58	5.34	5.16
TiO_2	0.35	0.12	0.28	0.25	0.24	0.25	0.46	0.42	0.27	0.33
P_2O_5	0.13	0.08	0.09	0.11	0.09	0.13	0.13	0.23	0.19	0.15
L. I.	1.12	0.42	1.43	0.99	0.73	0.75	0.71	0.71	0.64	0.71
Total	100.00	99.76	99.15	99.64	100.00	100.00	100.01	100.01	100.01	100.01
Q	194	266	234	231	217	207	228	207	236	220.00
P	15	33	-32	5	35	35	8	-9	42	20.00
A	58	67	79	68	42	41	47	38	62	47.00
B	71	27	68	55	43	40	76	69	44	57.00
Na+K	199	166	148	171	192	194	163	184	171	181.00
K/(Na+K)	0.56	0.61	0.49	0.55	0.61	0.63	0.59	0.53	0.66	0.61
Mg/(Mg+Fe)	0.36	0.34	0.55	0.42	0.25	0.37	0.41	0.40	0.35	0.36
Q%	34.90	47.90	42.20	41.67	39.00	37.40	41.00	37.30	42.60	39.46
B%	12.70	4.90	12.20	9.93	7.80	7.20	13.80	12.50	7.90	9.84
F%	52.40	47.20	45.60	48.40	53.20	55.40	45.20	50.20	49.50	50.70
Nomenclature	gr II	lc gr I	gr II	gr II	gr II	gr II	gr II	gr II	gr II	gr II

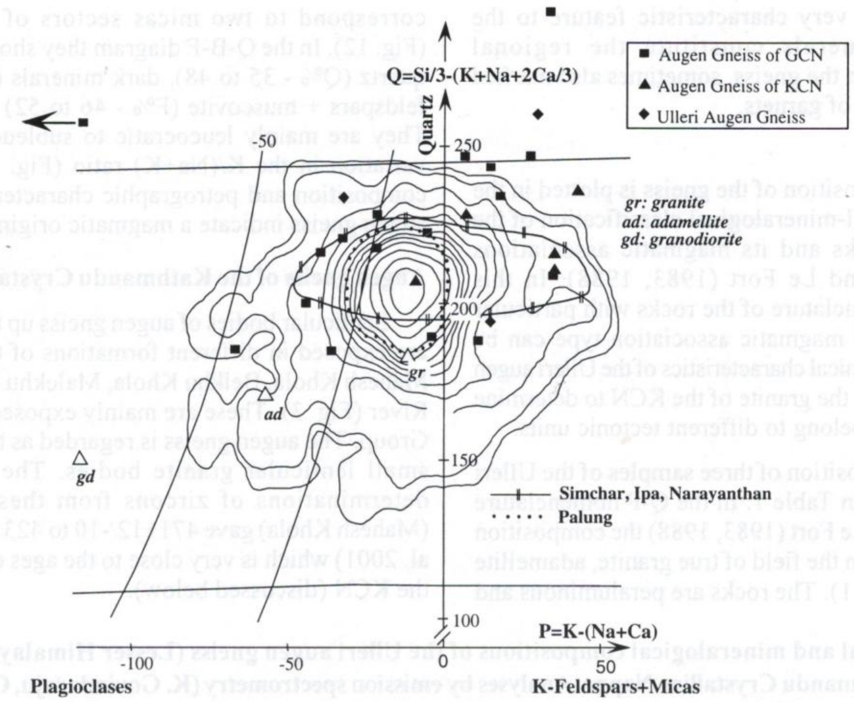

Fig. 11: Chemical composition of the augen gneiss of central Nepal (Ulleri augen gneiss, KCN and GCN) and the granites of the KCN (Simchar, Ipa, Narayan Than, Palung) in the Q-P diagram (after Debon and Le Fort 1983, 1988). For comparision, the distribution of granite of the KCN is represented by isodensity curve prepared by "Service d'Etudes Documentaires et Traitement Automatique" (E.D.T.A.) du C.R.P.G. de Nancy (after Le Fort et al. 1983).

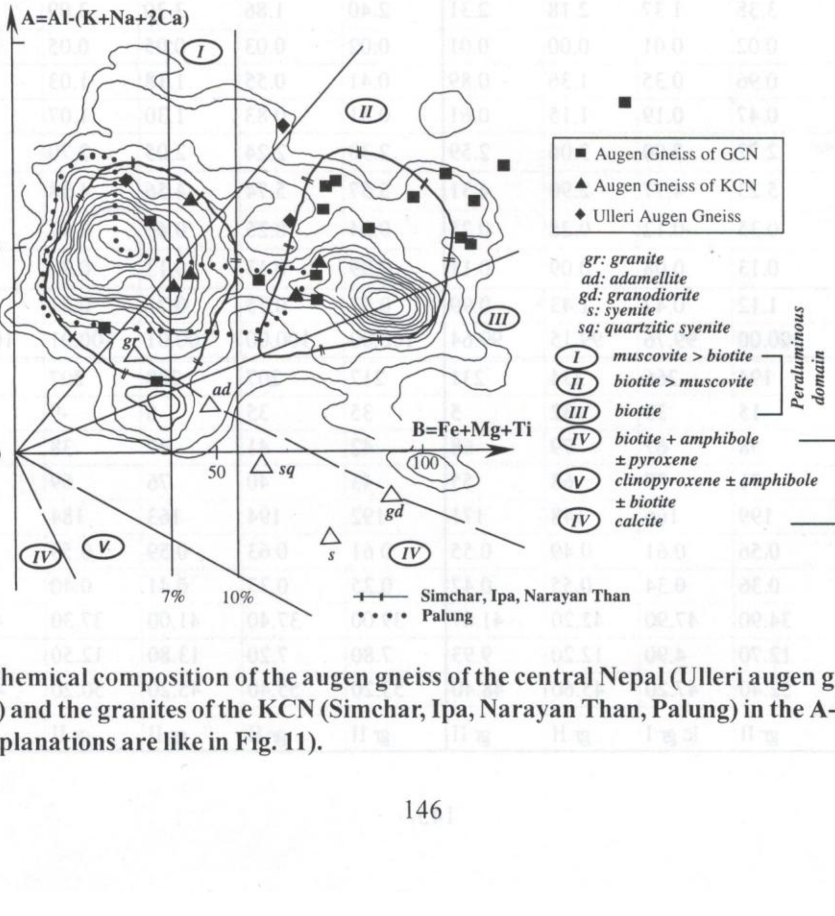

Fig. 12: Chemical composition of the augen gneiss of the central Nepal (Ulleri augen gneiss, KCN and GCN) and the granites of the KCN (Simchar, Ipa, Narayan Than, Palung) in the A-B diagram. (Other explanations are like in Fig. 11).

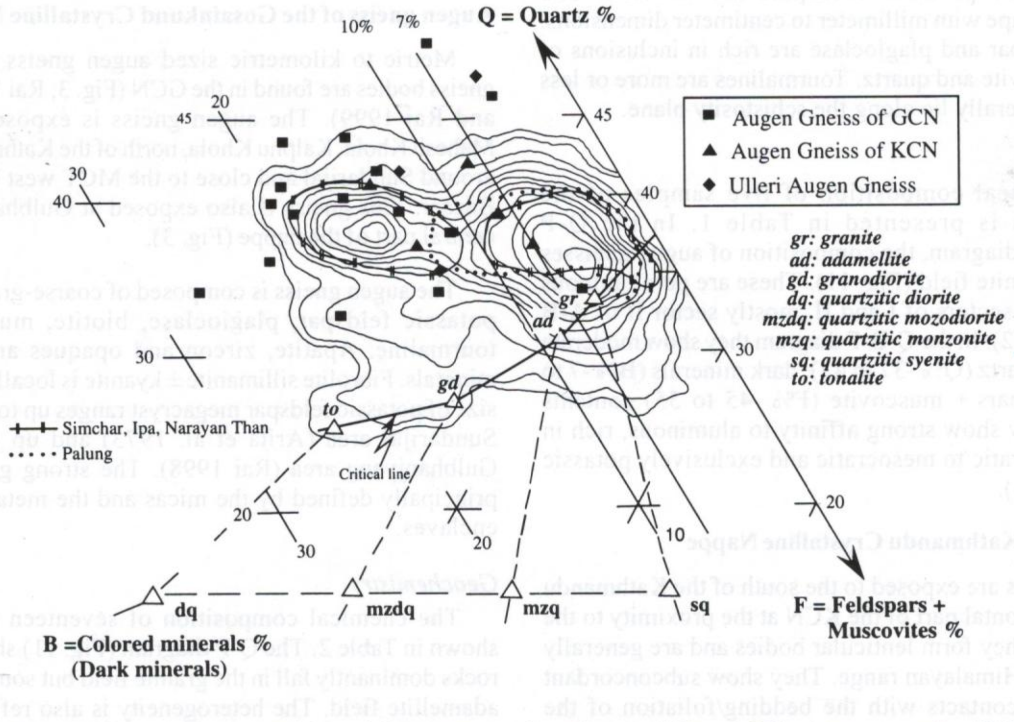

Fig. 13: Chemical composition of the augen gneiss of central Nepal (Ulleri augen gneiss, KCN and GCN) and the granites of the KCN (Simchar, Ipa, Narayan Than, Palung) in the Q-B-F diagram. Other explanations are like in Fig. 11.

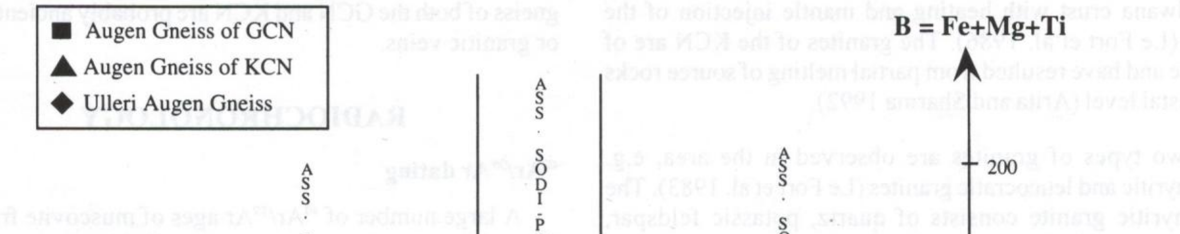

Fig. 14: Chemical composition of the augen gneiss of central Nepal (Ulleri augen gneiss, KCN and GCN) in the B-K/(Na+K) diagram (after Debon and Le Fort 1983, 1988).

The augen gneiss is comprised of potassic feldspar, quartz, plagioclase, biotite, muscovite and tourmaline. Coarse-grained potassic feldspars are ovoid to sub rectangular shape with millimeter to centimeter dimensions. Potassic feldspar and plagioclase are rich in inclusions of biotite, muscovite and quartz. Tourmalines are more or less zoned and generally lie along the schistosity plane.

Geochemistry

The chemical composition of five samples of the augen gneiss is presented in Table 1. In the Q-P nomenclature diagram, the composition of augen gneisses falls in the granite field (Fig. 11). These are peraluminous and fall in the sectors of I and II, mostly sector II of A-B diagram (Fig. 12). In the Q-B-F diagram they show moderate variation in quartz (Q% -37 to 43), dark minerals (B% -7 to 14) and feldspars + muscovite (F% -45 to 55) contents (Fig. 13). They show strong affinity to aluminous, rich in quartz, leucocratic to mesocratic and exclusively potassic granite (Fig. 14).

Granite of the Kathmandu Crystalline Nappe

The granites are exposed to the south of the Kathmandu Valley in the frontal part of the KCN at the proximity to the MT (Fig. 3). They form lenticular bodies and are generally parallel to the Himalayan range. They show subconcordant to discordant contacts with the bedding/foliation of the country rocks. The largest plutons are orthogneissified along their boarders under amphibolite facies (two micas + garnet) (Le Fort et al. 1983). The age of the granites is Cambro-Ordovician (Le Fort et al. 1981, 1983; Schärer and Allègre 1983). These granites were probably produced by large melting of the continental crust at the northern tip of the Indian craton during a general episode of thinning of Gondwana crust with heating and mantle injection of the crust (Le Fort et al. 1986). The granites of the KCN are of S-type and have resulted from partial melting of source rocks at crustal level (Arita and Sharma 1992).

Two types of granites are observed in the area, e.g. porphyritic and leucocratic granites (Le Fort et al. 1983). The porphyritic granite consists of quartz, potassic feldspar, plagioclase, biotite, muscovite, tourmaline, ± cordierite. Apatite, zircon and opaques are accessory minerals. The leucocratic granite is composed of quartz, potassic feldspar, plagioclase, biotite, muscovite, tourmaline, and cordierite with accessory minerals as garnet, apatite, zircon.

Geochemistry

Chemical analyses of 296 samples of granites from the KCN were used by Le Fort et al. (1983) to give nomenclature of the granites using the Q-P, A-B and Q-B-F diagrams. The composition of the KCN granites principally falls in the granite field (aluminous, rich in quartz) of Le Fort et al. (1983). This association is characterized by a bimodal distribution marked by the content of dark minerals that shows two maxima, one mesocrate and the other leucocrate (Fig. 12 and 13).

Augen gneiss of the Gosainkund Crystalline Nappe

Metric to kilometric sized augen gneiss and granitic gneiss bodies are found in the GCN (Fig. 3; Rai 1998; Le Fort and Rai 1999). The augen gneiss is exposed along the Mahesh Khola, Kalphu Khola, north of the Kathmandu Valley around Sundarijal and close to the MCT west of Melamchi Bazaar. This gneiss is also exposed at Gulbhanjyng in the central part of the nappe (Fig. 3).

The augen gneiss is composed of coarse-grained quartz, potassic feldspar, plagioclase, biotite, muscovite and tourmaline. Apatite, zircon and opaques are accessory minerals. Fibrolite sillimanite ± kyanite is locally found. The size of potassic feldspar megacryst ranges up to 18 cm in the Sundarijal area (Arita et al. 1973) and up to 10 cm in Gulbhanjyang area (Rai 1998). The strong gneissosity is principally defined by the micas and the metasedimentary enclaves.

Geochemistry

The chemical composition of seventeen samples are shown in Table 2. The Q-P diagram (Fig. 11) shows that the rocks dominantly fall in the granite field but some also fall in adamellite field. The heterogeneity is also reflected in the variation in K/(Na+K) ratio (Fig. 14). The analysed rocks are aluminous, principally fall within sectors I and II of A-B diagram (Fig. 12). In the Q-B-F diagram they show a variation in quartz (Q% = 34 to 45), dark minerals (B% = 4 to 27) and feldspar + muscovite (F%= 38 to 60) (Fig. 13). In general the gneiss shows an aluminous, quartz rich, mesocratic association and dominantly postassic (Fig. 14). The augen gneiss of both the GCN and KCN are probably ancient stocks or granitic veins.

RADIOCHRONOLOGY

$^{40}Ar/^{39}Ar$ dating

A large number of $^{40}Ar/^{39}Ar$ ages of muscovite from the LH, KCN and GCN were determined (Rai 1998; Copeland et al. in press). The analyses were carried out by Dr. Peter Copeland in the Department of Geosciences, University of Houston, USA. The results are further discussed in a separate paper (Copeland et al. in press, Tectonics).

The $^{40}Ar/^{39}Ar$ ages of muscovite in the Lesser Himalaya vary from 12 Ma (away from the MCT) to 6 Ma (near the MCT) (Fig. 15). The ages in the KCN systematically decrease from 22 Ma in the south near the MT to 14 Ma near the MCT, north of the Kathmandu Valley (Fig. 15 and 16). These age distributions do not correspond with the present topography but are systematically younging from south to the north. Also, the cooling ages do not show any relation with respect

Table 2: Chemical and mineralogical compositions of the augen gneiss of the Gosainkund Crystalline Nappe. Analyses by XRF at Geoscience Laboratory, GSP, Islamabad, Pakistan except samples KN29, KN47 and KN109 (emission spectrometry, CRPG, Nancy) (Le Fort and Rai 1999). The parameters and topology are based on Debon and Le Fort (1983, 1988).

Sample number	KN29	KN41	KN47	KN109	KN250	KN255	KN256	KN467	KN471	KN482	KN491	KN543	KN557	KN572	KN578	KN585	KN620	average
SiO_2	71.64	70.67	73.81	68.21	73.39	78.58	70.91	73.43	71.30	73.54	72.78	77.98	73.19	70.36	67.46	72.83	64.55	72.04
Al_2O_3	13.55	13.48	13.36	14.78	13.37	12.59	14.23	13.11	13.64	12.98	13.56	11.88	13.42	13.52	15.26	12.83	16.44	13.65
Fe_2O_3t	4.03	4.96	2.13	4.83	2.71	0.99	3.38	3.41	4.61	3.39	3.45	1.55	3.57	4.87	5.58	4.21	6.20	3.76
MnO	0.05	0.04	0.02	0.05	0.03	0.02	0.05	0.05	0.08	0.05	0.05	0.03	0.04	0.07	0.07	0.06	0.08	0.05
MgO	1.20	1.75	0.23	1.66	0.84	0.34	1.08	1.02	1.63	1.14	1.01	0.47	1.12	1.67	1.61	1.53	2.44	1.22
CaO	1.41	1.18	0.99	1.85	0.92	1.53	1.43	1.05	1.33	1.20	1.34	0.70	1.48	1.91	2.32	1.32	2.75	1.45
Na_2O	2.60	2.78	3.03	3.17	2.18	4.29	2.36	1.90	2.31	1.51	2.61	1.14	1.60	1.80	2.32	1.72	1.93	2.31
K_2O	3.60	3.34	5.24	3.23	5.45	1.08	5.29	4.64	3.64	4.63	4.08	5.38	4.39	4.12	3.40	4.08	3.61	4.07
TiO_2	0.55	0.62	0.21	0.67	0.41	0.14	0.49	0.53	0.65	0.49	0.51	0.22	0.50	0.75	0.78	0.59	0.87	0.53
P_2O_5	0.15	0.10	0.06	0.17	0.09	0.05	0.13	0.14	0.11	0.14	0.11	0.09	0.10	0.16	0.30	0.19	0.13	0.13
L. I.	1.07	0.90	0.75	1.15	0.61	0.41	0.65	0.71	0.71	0.93	0.51	0.55	0.60	0.77	0.89	0.64	1.00	0.76
Total	99.85	99.82	99.83	99.77	99.99	100.02	100.01	99.99	100.01	100.01	100.01	99.99	100.02	100.00	100.00	100.00	100.00	99.96
Q	221	218	189	186	210	257	188	235	228	247	217	273	244	222	200	246	187	222
P	-33	-40	-4	-67	29	-143	11	19	-21	28	-21	65	15	-5	-44	8	-35	-14
A	55	62	18	53	43	31	40	60	68	65	47	57	66	52	70	63	86	55
B	87	113	35	110	60	23	75	75	106	77	75	34	79	112	120	98	149	84
Na+K	160	161	209	171	186	161	188	160	152	147	171	151	145	146	147	142	138	161
K/(Na+K)	0.48	0.44	0.53	0.40	0.62	0.14	0.60	0.62	0.51	0.67	0.51	0.76	0.64	0.60	0.49	0.61	0.55	0.54
Mg/(Mg+Fe)	0.37	0.41	0.18	0.40	0.38	0.40	0.39	0.37	0.41	0.40	0.37	0.38	0.38	0.40	0.36	0.42	0.44	0.38
Q%	39.70	39.20	34.00	33.50	37.90	46.00	33.90	42.40	41.10	44.50	39.10	49.30	43.90	40.00	36.00	44.40	33.70	40.00
B%	15.70	20.40	6.30	19.80	10.80	4.00	13.60	13.50	19.10	13.80	13.50	6.10	14.20	20.20	21.50	17.70	26.80	15.00
F%	44.60	40.40	59.70	46.70	51.30	50.00	52.50	44.10	39.80	41.70	47.40	44.60	41.90	39.80	42.50	37.90	39.50	45.00
Nomenclature	ad II	ad II	lc gr II	ad II	gr II	lc to I	gr II	gr II	ad II	gr II	gr II	lc gr I	gr I	gr I	ad I	gr II	ad II	gr II

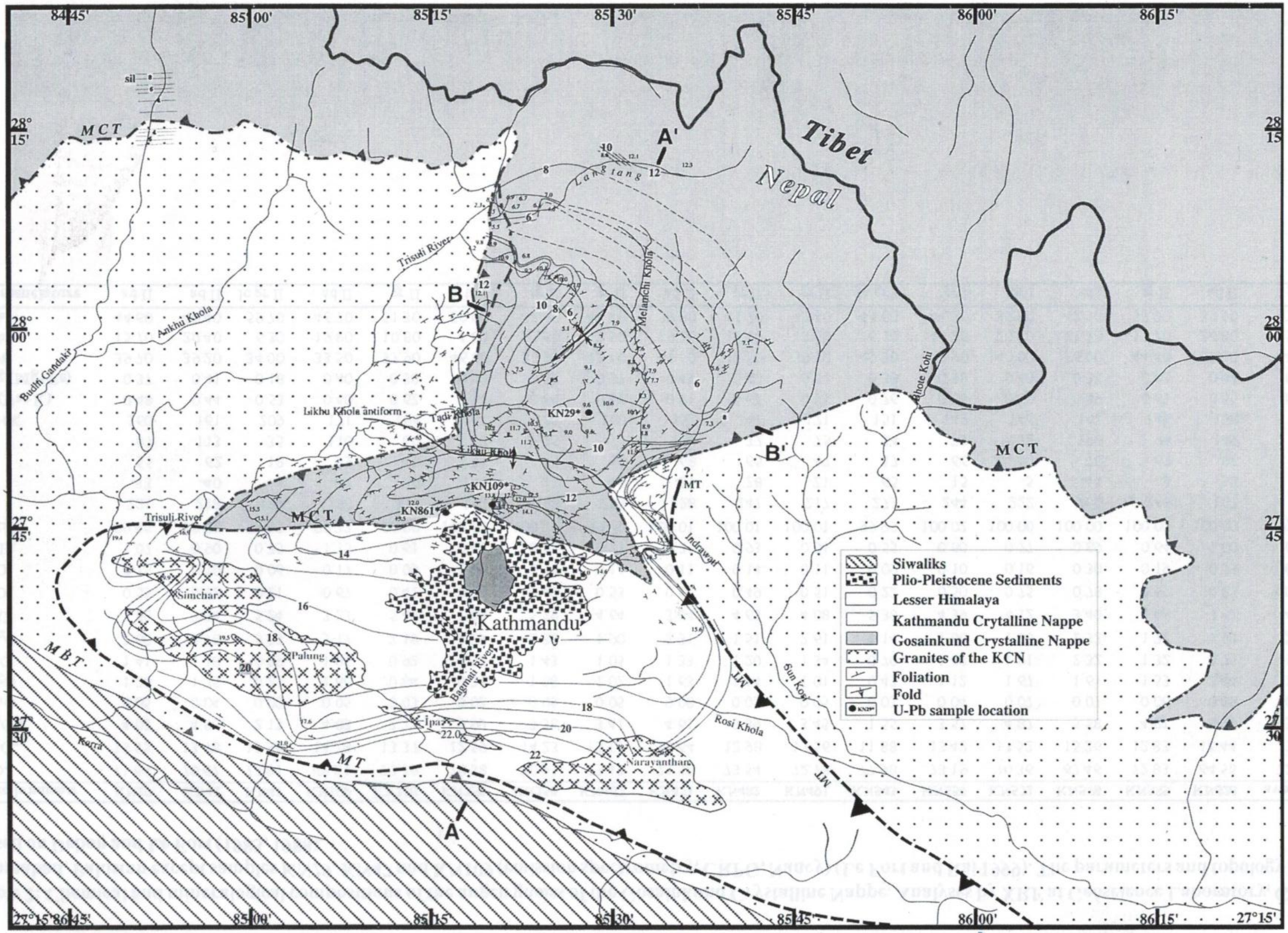

Fig. 15: Distribution of $^{40}Ar/^{39}Ar$ ages in muscovite in the study area (Lesser Himalaya, Kathmandu Crystalline Nappe and Gosainkund Crystalline Nappe) with isochrone curves. A-A' and B-B' represent the cross-sections shown in Fig. 16. KN29*, KN109* and KN861* are the sample locations for U-Pb dating. MBT: Main Boundary Thrust, MCT: Main Central Thrust, MT: Mahabharat Thrust.

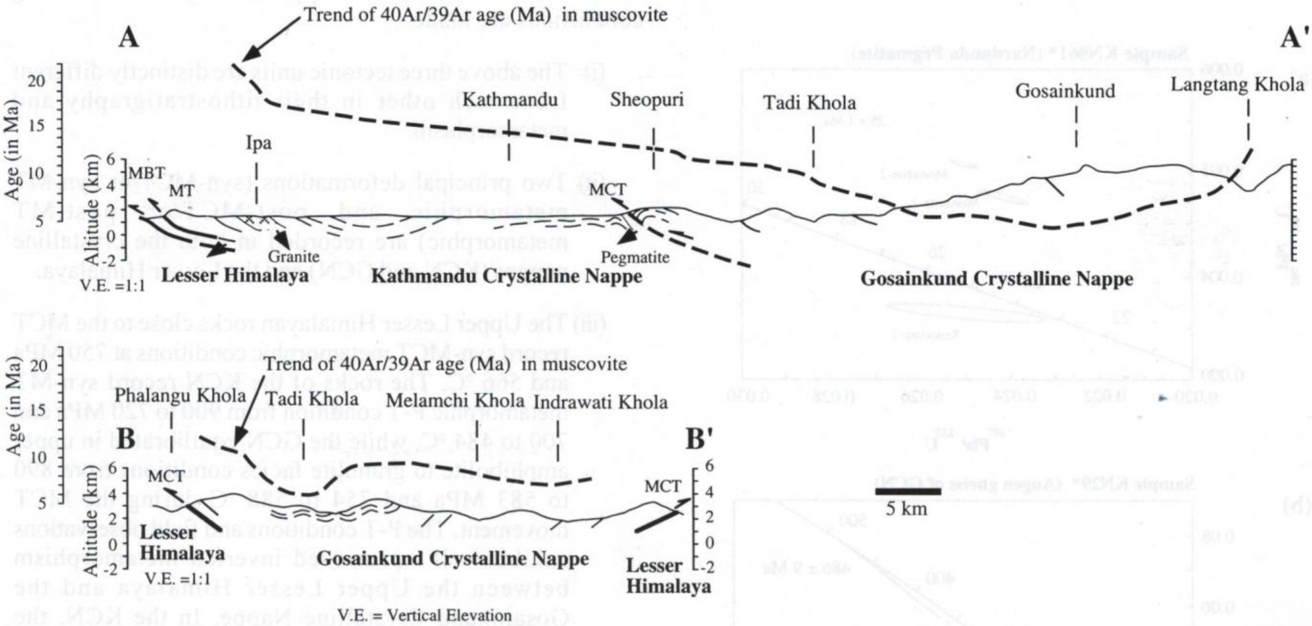

Fig. 16: Distribution of the $^{40}Ar/^{39}Ar$ ages in muscovites across the sections (Fig. 15) (Copeland et al. in press). MBT: Main Boundary Thrust, MCT: Main Central Thrust, MT: Mahabharat Thrust.

to the lithology or stratigraphy of the rocks. The oldest age (22 Ma) is recorded from the Ipa granite located at the southern front within the KCN.

As in case of the KCN, the $^{40}Ar/^{39}Ar$ ages in the GCN also show a systematic decrease from south to north (from 16 to 5 Ma) and do not show any relation with topographic elevation or with structural distance from the MCT (Fig. 15 and 16).

The systematic decrease of cooling ages from south to north recorded in both KCN and GCN corresponds to a younger structure or late deformation (flexure of the MCT over the MBT (Macfarlane 1993; Copeland et al. 1997). This pattern of cooling ages suggests that the exhumation of the GCN resulted from the flexure of the Himalayan décollement over MBT (Pandey et al. 1995). The older ages recorded in the KCN than those in the GCN suggest that the rock of the KCN along the MT was exhumed prior to that of the rocks of the GCN along the MCT. It suggests that both nappes progressively moved to south over a ramp structure.

U-Pb dating

Zircon, monazite and xenotime from the Nardanda pegmatite of the KCN and zircon and monazite from augen gneisses from Gulbhanjyang area (GCN) and the southern front of the GCN (Fig. 15) were dated by U-Pb method (Rai 1998). The analyses were carried out by Dr. R. Parrish in the Laboratory of NERC, Isotope Geoscience Centre, UK. The results are discussed in more detail in a separate paper (Copeland et al. in press).

Nardanda pegmatite

Both monazite and xenotime in the pegmatite show similar ages around 25±1 Ma (Fig. 17a) which correspond to the crystallisation age of the pegmatite. The age of the Nardanda pegmatite appears to be older than those of the leucogranites of the Higher Himalaya (24.0 to 17.2 Ma; Deniel et al. 1987; Harrison 1999) situated about 60 km to the north.

Augen gneiss of the Gosainkund Crystalline Nappe

An Early-Ordovician age (486 ± 9 Ma) obtained from zircon (Fig. 17b) in the augen gneiss, near the Gulbhajyang Village of the GCN is very close to the ages obtained from the augen gneiss of the Higher Himalayan Crystallines in the root zone (Le Fort et al. 1982; Hodges et al. 1996) and the ages obtained from the granites of KCN (Schärer and Allègre 1983; Le Fort et al. 1983). The coarse - grained augen gneiss of the Formation III of the Higher Himalayan Crystallines or the Tibetan Slab west of the present study area also showed the Rb-Sr whole rock age of 513 ± 30 Ma (Le Fort et al. 1986). Thus the two augen gneisses may be regarded as the contemporaneous magmatic events.

The 26 to 27 Ma age of monazite crystals from the augen gneiss of the GCN at the proximity of the MCT (north of the Kathmandu Valley) and lying about 5 km north of the Nardanda Pegmatite (Fig. 17c) is highly contrasting with the age of the augen gneiss of Gulbhanjyang (486 ± 9 Ma), though they belong to the same tectonic unit and have the same petrographic and geochemical characteristics. This young age may be interpreted as the imprint of the young Himalayan metamorphism over the older augen gneiss.

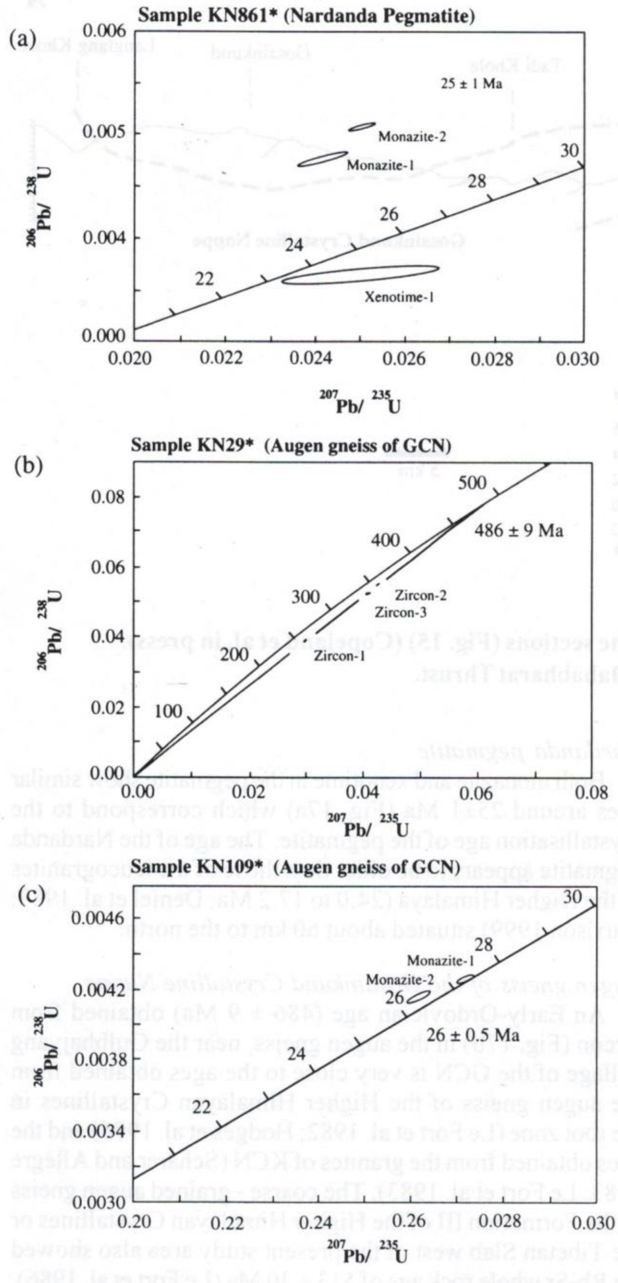

Fig. 17: Concordia diagram for U-Pb (Copeland et al., in press). Sample locations are shown in Fig. 15.
a: Nardanda Pegmatite (monazite and xenotime crystals).
b: Augen gneiss of the GCN (zircon crystals).
c: Augen gneiss of the GCN (monazite crystals).

CONCLUSIONS

Based on the structural, metamorphic, geochemical and radiochronological studies of the Lesser Himalaya (LH), Kathmandu Crystalline Nappe (KCN) and Gosainkund Crystalline Nappe (GCN) the following conclusions are made:

(i) The above three tectonic units are distinctly different from each other in their lithostratigraphy and metamorphism.

(ii) Two principal deformations (syn-MCT/or syn-MT metamorphic and post-MCT/or post-MT metamorphic) are recorded in both the crystalline nappes (KCN and GCN) and the Lesser Himalaya.

(iii) The Upper Lesser Himalayan rocks close to the MCT record syn-MCT metamorphic conditions at 750 MPa and 566 °C. The rocks of the KCN record syn-MT metamorphic P-T condition from 900 to 720 MPa and 700 to 484 °C, while the GCN equilibrated in upper amphibolite to granulite facies conditions from 890 to 583 MPa and 754 to 588 °C during the MCT movement. The P-T conditions and field observations exhibit well - preserved inverted metamorphism between the Upper Lesser Himalaya and the Gosainkund Crystalline Nappe. In the KCN, the estimated temperature is lower by about 100°C than observed in the GCN, whereas the pressure remains at about 800 MPa in both the nappes.

(iv) The 486±9 Ma U-Pb zircon age of the augen gneiss from the GCN is similar to previously reported method ages of granites from the KCN. The geochemical characteristics of the augen gneiss of the GCN and KCN, granites of the KCN and the Ulleri augen gneiss of the LH show close similarity. The chemical analyses of both the Proterozoic Ulleri augen gneiss of the LH and the granite of the KCN fall in the same compositional field. It indicates that the augen gneiss is also of magmatic origin.

(v) The systematic decrease of $^{40}Ar/^{39}Ar$ ages of muscovite from south to north recorded in both the KCN and GCN corresponds to a younger structure or late deformation. So both the KCN and the GCN record a late emplacement history, but the KCN was exhumed earlier than the GCN. Both crystalline nappes (KCN and GCN) presently form a single tectonic block, and the combined uplift of the two nappes occurs on a ramp of a major décollement formed at the upper part of the Indian crust (Fig. 18).

ACKNOWLEDGEMENTS

I would like to express my special thanks to Drs. P. Le Fort, B. N. Upreti, S. Guillot, A. Pêcher, F. Debon, P. Copeland, and R. Parrish for their valuable guidance and help during the course of this study. The author also wishes to express his sincere thanks to Dr. K. Arita for providing helpful and valuable comments on the first version of the manuscript. I am highly thankful to Dr. B. N. Upreti for fruitful discussions and improvement of the final draft of the manuscript. Field

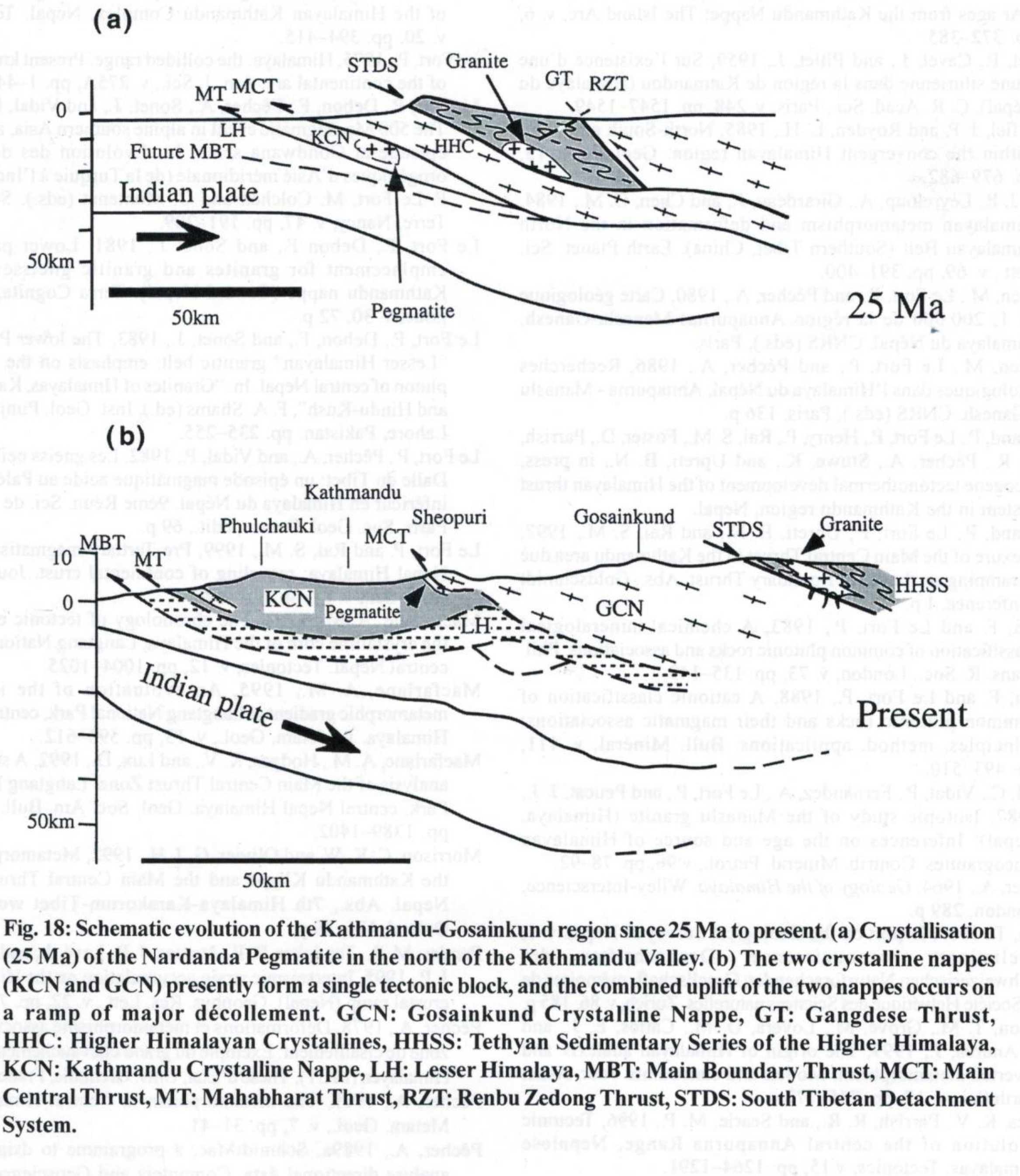

Fig. 18: Schematic evolution of the Kathmandu-Gosainkund region since 25 Ma to present. (a) Crystallisation (25 Ma) of the Nardanda Pegmatite in the north of the Kathmandu Valley. (b) The two crystalline nappes (KCN and GCN) presently form a single tectonic block, and the combined uplift of the two nappes occurs on a ramp of major décollement. GCN: Gosainkund Crystalline Nappe, GT: Gangdese Thrust, HHC: Higher Himalayan Crystallines, HHSS: Tethyan Sedimentary Series of the Higher Himalaya, KCN: Kathmandu Crystalline Nappe, LH: Lesser Himalaya, MBT: Main Boundary Thrust, MCT: Main Central Thrust, MT: Mahabharat Thrust, RZT: Renbu Zedong Thrust, STDS: South Tibetan Detachment System.

works for this research was supported by IDYLHIM project organized by Dr. P. Le Fort, Directeur de Recherches, CNRS, France and Main Himalayan Thrust project organized by Dr. Harutaka Sakai, Kyushu university, Japan to whom the author is highly indebted. I am grateful to the Government of France for providing me scholarship to carry out research leading to Ph.D. at the Université Joseph Fourier, Grenoble, France.

REFERENCES

Arita, K., Ohta, Y., Akiba, C., and Maruo, Y., 1973, Kathmandu Region. In: Geology of the Nepal Himalayas. Hashimoto S., Ohta Y., and Akiba C. (eds.) Tokyo, Saikon Publishing Co. Ltd., 286 p.

Arita, K. and Sharma, M. P., 1992, Chemical characteristics of some granitic rocks in central Nepal. Bull. Dept. Geology, Tribhuvan Univ., Kathmandu, v. 2(1), pp. 1–9.

Arita, K., Dallmeyer, R. D., and Takasu, A., 1997, Tectonothermal evolution of the Lesser Himalaya, Nepal: Constraints $^{40}Ar/^{39}Ar$ ages from the Kathmandu Nappe: The Island Arc, v. 6, pp. 372–385.

Bordet, P., Cavet, J., and Pillet, J., 1959, Sur l'existence d'une faune silurienne dans la région de Katmandou (Himalaya du Népal). C. R. Acad. Sci., Paris, v. 248, pp. 1547–1549.

Burchfiel, J. P. and Royden, L. H., 1985, North-South extension within the convergent Himalayan region. Geology, v. 13, pp. 679–682.

Burg, J. P., Leyreloup, A., Girardeau, J., and Chen, G. M., 1984, Himalayan metamorphism and deformation in the North Himalayan Belt (Southern Tibet, China). Earth Planet. Sci. Lett., v. 69, pp. 391–400.

Colchen, M., Le Fort, P., and Pêcher, A., 1980, Carte géologique au 1: 200.000 de la région Annapurnas-Manaslu-Ganesh, Himalaya du Népal. CNRS (eds.), Paris.

Colchen, M., Le Fort, P., and Pêcher, A., 1986, Recherches géologiques dans l'Himalaya du Népal. Annapurna - Manaslu - Ganesh. CNRS (eds.), Paris, 136 p.

Copeland, P., Le Fort, P., Henry, P., Rai, S. M., Foster, D., Parrish, R. R., Pêcher, A., Stuwe, K., and Upreti, B. N., in press, Neogene tectonothermal development of the Himalayan thrust system in the Kathmandu region, Nepal.

Copeland, P., Le Fort, P., Upreti, B. N., and Rai, S. M., 1997, Flexure of the Main Central Thrust in the Kathmandu area due to ramping on the Main Boundary Thrust. Abs., Goldschmidt conference, 1 p.

Debon, F. and Le Fort, P., 1983, A chemical-mineralogical classification of common plutonic rocks and associations. Phil. Trans. R. Soc., London, v. 73, pp. 135–149.

Debon, F. and Le Fort, P., 1988, A cationic classification of common plutonic rocks and their magmatic associations: principles, method, applications. Bull. Minéral, v. 111, pp. 493–510.

Deniel, C., Vidal, P., Fernandez, A., Le Fort, P., and Peucat, J. J., 1987, Isotopic study of the Manaslu granite (Himalaya, Nepal): Inferences on the age and source of Himalayan leucogranites. Contrib. Mineral. Petrol., v 96, pp. 78–92.

Gansser, A., 1964, *Geology of the Himalaya.* Wiley-Interscience, London, 289 p.

Hagen, T., 1969, Report on the Geological Survey of Nepal. v. 1, Preliminary reconnaissance. Denkschriften der Schweizerischen Naturforschenden Gesellschaft, mémoires de la Société Helvétique des Sciences naturelles, Zurich, v. 86, 185 p.

Harrison, T. M., Grove, M., Lovera, O. M., Catlos, E. J., and D'Andrea, J., 1999, The origin of Himalayan anatexix and inverted metamorphism: Models and constraints. Jour. Asian Earth Sci., v. 17, pp. 755–772.

Hodges, K. V., Parrish, R. R., and Searle, M. P., 1996, Tectonic evolution of the central Annapurna Range, Nepalese Himalayas. Tectonics, v.15, pp. 1264–1291.

Holland, T. J. B. and Powell, R., 1990, An enlarged and updated internally consistent thermodynamic dataset with uncertainties and correlations: the system K_2O-Na_2O-Cao-MgO-Fe_2O_3-Al_2O_3-TiO_2-SiO_2-C-H_2-O_2. Jour. Metam. Geol., v. 8, pp. 89–124.

Inger, S., 1991, Metamorphism and granite genesis in the Langtang region, North-Central Nepal. Ph.D. Thesis, Open University, UK, 272 p.

Johnson, M. R. W. and Rogers, G., 1997, Rb-Sr ages of micas from the Kathmandu complex, Central Nepalese Himalaya: implications for the evolution of the Main Central Thrust. J. Geol. Soc., London, v. 154, pp. 863–869.

Johnson, M. R. W., Oliver, G. J. H., Parrish, R. R., and Johnson, S. P., 2001, Synthrusting metamorphism, cooling, and erosion of the Himalayan Kathmandu Complex, Nepal. Tectonics, v. 20, pp. 394–415.

Le Fort, P., 1975, Himalaya: the collided range. Present knowledge of the continental arc. Am. J. Sci., v. 275A, pp. 1–44.

Le Fort, P., Debon, F., Pêcher, A., Sonet, J., and Vidal, P., 1986, The 500 Ma magmatic event in alpine southern Asia, a thermal episode at Gondwana scale. In: Evolution des domaines orogéniques d'Asie méridionale (de la Turquie à l'Indonésie), P. Le Fort, M. Colchen and C. Montenat (eds.), Sci. de la Terre, Nancy, v. 47, pp. 191–209.

Le Fort, P., Debon F., and Sonet J., 1981, Lower paleozoic emplacement for granites and granitic gneisses of the Kathmandu nappe (Central Nepal). Terra Cognita, special issue, v. 30, 72 p.

Le Fort, P., Debon, F., and Sonet, J., 1983, The lower Palaozoic "Lesser Himalayan" granitic belt: emphasis on the Simchar pluton of central Nepal. In: "Granites of Himalayas, Karakorum and Hindu-Kush", F. A. Shams (ed.), Inst. Geol. Punjab univ., Lahore, Pakistan. pp. 235–255.

Le Fort, P., Pêcher, A., and Vidal, P., 1982, Les gneiss oeillés de la Dalle du Tibet: un épisode magmatique acide au Paléozoïque inférieur en Himalaya du Népal. 9ème Réun. Sci. de la Terre, Paris, Soc. Geol. France, édit., 69 p.

Le Fort, P. and Rai, S. M., 1999, Pre-Tertiary magmatism of the Nepal Himalaya: recycling of continental crust. Jour. Asian Earth Sci., v. 17, pp. 607–628.

Macfarlane, A. M., 1993, The chronology of tectonic events in the crystalline core of the Himalaya, Langtang National Park, central Nepal. Tectonics, v. 12, pp. 1004–1025.

Macfarlane, A. M., 1995, An evoluation of the inverted metamorphic gradient at Langtang National Park, central Nepal Himalaya. J. Metam. Geol., v. 13, pp. 595–612.

Macfarlane, A. M., Hodges, K. V., and Lux, D., 1992, A structural analysis of the Main Central Thrust Zone, Langtang National Park, central Nepal Himalaya. Geol. Soc. Am. Bull., v. 104, pp. 1389–1402.

Morrison, C. K. W. and Olivier, G. J. H., 1992, Metamorphism in the Kathmandu Klippe and the Main Central Thrust zone, Nepal. Abs., 7th Himalaya-Karakorum-Tibet workshop, Oxford, UK, 59 p.

Pandey, M. R., Tandukar, R. P., Avouac, J. P., Lavé, J., and Massot, J. P., 1995, Interseismic strain accumulation on the Himalayan crustal ramp (Nepal). Geophys. Res. Lett., v. 22, pp. 751–754.

Pêcher, A., 1978, Déformations et métamorphisme associés à une zone de cisaillement: Exemple du grand chevauchement central Himalayen (MCT), Thèse d'Etat, Univ. Grenoble, France, 354 p.

Pêcher, A., 1989, The metamorphism in Central Himalaya. J. Metam. Geol., v. 7, pp. 31–41.

Pêcher, A., 1989a, SchmidtMac, a programme to dsiplay and analyse directional data. Computers and Geoscience. v. 15, pp. 1326–1345.

Pêcher, A., 1991, The contact between the Higher Himalayan Crystallines and the Tibetan Sedimentary Series: Miocene large scale dextral shearing. Tectonics, v. 10, pp. 587–598.

Pêcher, A. and Le Fort, P., 1986, The metamorphism in central Himalaya: its relations with the thrust tectonics. In: Evolution des domaines orogéniques d'Asie méridionale (de la Turquie à l'Indonésie), P. Le Fort, M. Colchen, and C. Montenat (eds.), Sci. de la Terre, Nancy, France, v. 47, pp. 285–309.

Rai, S. M., 1998, Les nappes de Katmandou et du Gosainkund, Himalaya du Népal central (étude cartographique, structurale, métamorphique, géochimique et radiochronologique). Ph.D. Thesis, Joseph Fourier University, Grenoble, France, 244 p.

Rai, S. M., Guillot, S., and Le Fort, P., 1997a, Pressure-temperature evolution in the Kathmandu and Gosainkund crystalline nappes (central Nepal). Abs., 12th Himalaya-Karakorum-Tibet Intl. workshop, Roma, Italy, pp. 195–196.

Rai, S. M., Le Fort, P., and Upreti, B. N., 1997b, Geology, structure and metamorphism in Kathmandu and Gosainkund regions, central Nepal. Abs., Jour. Nepal Geol. Soc. Spec. Pub., v. 16, pp. 20–22.

Rai, S. M., Guillot, S., Le Fort, P., and Upreti, B. N., 1998a, Mineral chemistry and tectonothermal evolution of the crystalline sheets in the Kathmandu region, central Nepal: Relation to geodynamic context. Abs., 13th Himalaya-Karakorum-Tibet Intl. workshop, Peshawar, Pakistan, pp. 157–159.

Rai, S. M., Guillot, S., Le Fort, P., and Upreti, B. N., 1998b, Evolution P-T des régions de Katmandou et du Gosainkund, Népal central. Résumé, Réunion des Sci. de la Terre, Brest, France, pp. 181.

Rai, S.M., Guillot, S., Le Fort, P. and Upreti, B. N., 1998c, Pressure-temperature evolution in the Kathmandu and Gosainkund regions, Central Nepal. Jour. Asian Earth Sci., v. 16(2-3), pp. 283–298.

Reddy, S. M., Searle, M. P., and Massey, J. A., 1993, Structural evolution of the High Himalayan Gneiss sequence, Langtang Valley, Nepal. Jour. Geol. Soc., London, Spec. Pub., v. 74, pp. 375–389.

Schärer, U. and Allègre, C. J., 1983, The Palung granite (Himalaya); high-resolution U-Pb systematics in zircon and monazite. Earth Planet. Sci. Lett., v. 63, pp. 423–432.

Schelling, D. and Arita, K., 1991, Thrust tectonics, crustal shortening, and the structure of the far-eastern Nepal Himalaya. Tectonics, v. 10, pp. 851–862.

Stöcklin, J., 1980, Geology of the Nepal and its regional frame. Jour. Geol. Soc., London, v. 137, pp. 1–34.

Stöcklin, J. and Bhattarai, K. D., 1977, Geology of Kathmandu area and central Mahabharat Range, Nepal Himalaya. HMG Nepal/UNDP report, 64 p.

Upreti, B. N. and Le Fort, P., 1999, Lesser Himalayan Crystalline Nappes of Nepal: problem of their origin. Geol. Soc. Am. Bull. Spec. Pap., v. 328, pp. 225–238.

Upreti, B. N., 1999, An Overview of the stratigraphy and tectonics of Nepal Himalaya. Jour. Asian Earth Sci., v. 17, pp. 577–606.